ISSN (Print) 1226-1750
ISSN (Online) 2233-6656
Journal of Magnetics 25(1), 64-69 (2020) https://doi.org/10.4283/JMAG.2020.25.1.064

Optimal Design and Static Performance Analysis of Permanent Magnet Coupling for Chemical Pump Application

Se-hyun Rhyu[1], Salman Khaliq[1]*, Chan-Wook Baek[2], and Yeon-Chul Ha[3]

[1]*Intelligent Mechatronics Research Center, Korea Electronics Technology Institute (KETI), Korea*
[2]*Department of Naval Architecture and Ocean Engineering, Pusan National University, Korea*
[3]*The Korea Ship and Offshore Research Institute, Pusan National University, Korea*

(Received 14 October 2019, Received in final form 10 March 2020, Accepted 11 March 2020)

Magnetic couplings are considered suitable for many industrial applications where a separation is required between the driver and the driven. Utilizing magnetic couplings allows the transmission of torque without any mechanical contact. Generally, permanent magnets (PMs) are utilized in magnetic couplings instead of electromagnets to avoid extra circuitry. Accurate design and analysis of magnetic coupling are essential to reduce the PM volume for the required output performance. 3D finite element method (FEM) is considered the most accurate as it takes into account the end effects, which arises due to a shorter stack length as compared to the diameter of the coupling. In this paper, a permanent magnet coupling (PMC) is designed and optimized to be installed in a chemical pump that is handling high-temperature fluid. A prototype was also manufactured and tested in the laboratory to verify the analysis.

Keywords : Magnetic coupling, optimization, prototype

1. Introduction

Permanent magnet couplings (PMC) are electromechanical devices that are utilized to transmit torque without the mechanical connection between the two parts. There are two parts in a magnetic coupling i.e. driver and follower, and both parts are present in different parts of machinery creating a separation wall. Such arrangements are well suited to avoid hazardous or corrosive elements to interact with the machinery parts. Fig. 1 shows the structure of a radial-flux type PMC. Primary shaft mover is connected with the driving motor while the secondary follower shaft is connected to the pump load. One more advantage of the magnetic coupling is its inherent overload protection capacity in which the couplings part slip over each other due to overload, and can be used to avoid mechanical failure [1]. With such advantages, magnetic couplings can be applied in various applications such as clean room and non-contact power transmission separated by a vacuum.

Generally, it is required to obtain a specific torque output from the magnetic coupling with minimum magnet volume considering the required constraints. Therefore, the selection of optimum dimension leads to overall cost minimization while fulfilling the torque requirements of the system.

Due to non-linearity of the magnetic circuit and three-dimensional field nature, magnetic coupling design is complicated. In literature, analytical designs have been devised and utilized for the dimensions of the magnetic couplings. Such analytical approaches save time; however, they do not consider the leakage flux effect which becomes more prominent as the stack length of the coupling is

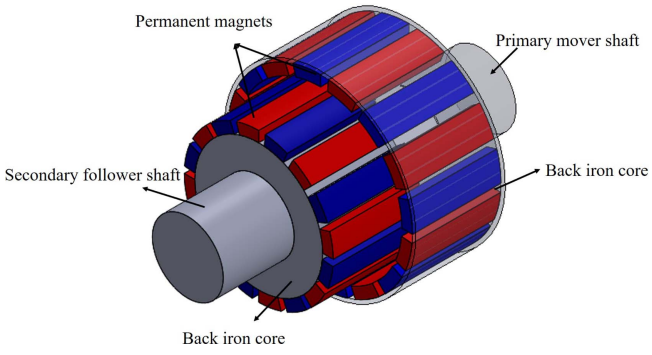

Fig. 1. (Color online) Structure of radial PMC.

*Corresponding author: Tel: +82-32-621-2848
Fax: +82-32-621-2855, e-mail: salman.khaliq@hotmail.com

reduced [2-4]. Furthermore, such analysis is unable to consider the unique structures in which the coupling is to be installed.

Fast computing finite element analysis (FEA) is used extensively for designing and analysis due to their high reliability [1]. Generally, air gap length is quite large i.e. 10 mm or larger, between the outer and inner rotating parts of the coupling. Therefore, leakage flux is present at the end part of the coupling. 2D FEA does not consider the leakage flux and causes trial and error experimental design approach. Whereas, 3D FEA considers the end effect, the unconventional structure and removes the effect of empirical factors [5-7].

PMC research in the literature is mainly focused on assessing the static performance and achieving the maximum output torque with as little of PM volume as possible. Several papers have analyzed magnetic couplings analytically with finite element method; however, most of these researches is not verified with experiments [8-11]. In addition, they rarely consider the industrial scale utilization of such couplings.

In this paper, 3D FEA is utilized to design and optimize the magnetic coupling for a chemical pump application. The PMC parts that is exposed to the chemical fluid are coated with a layer of Teflon to avoid the reaction of the fluid with the assembly. The pump is required to handle the fluid at a higher temperature, i.e. 150 °C; therefore, magnetic coupling is utilized to create a separation between the primary mover and the secondary follower. Inner diameter of the inner PMs, and air gap length were fixed due to the dimension constraints of the pump assembly. Then, the genetic algorithm is utilized to find the optimal dimension of the PMs to produce the required torque output. Finally, a prototype was manufactured and tested in the laboratory to verify the FEA results.

2. Permanent Magnet Coupling

A PMC consists of two parts: a primary driver and a secondary follower. Primary driver is connected to the driving motor which in this case is an induction motor (IM) and the secondary follower is connected to the pump impeller which is used for pumping chemical liquid. Static torque, τ_s is transmitted through the air gap between the two parts, which in this case is decided to be 14 mm to accommodate the assembly features and Teflon coating on the PMs. During no load condition, static torque transfer is zero and opposite poles of the primary driver and secondary follower face each other. However, as the load is increased on the secondary follower, the mechanical angle θ_m, between the two parts is increased and achieves a maximum value at 90 electrical degrees θ_e, which is obtained by multiplying mechanical degrees with the number of poles [8]. This maximum torque is termed as pullout torque, τ_{po} of the magnetic coupling and is written as:

$$\tau_e = \tau_{po} \sin\theta_e \tag{1}$$

Table 1. PMC Dimension Specifications and Operating Conditions.

Item	Value
Primary mover outer diameter [mm]	172
Secondary follower PM inner diameter [mm]	94
Separation wall distance [mm]	14
Maximum operating temperature [°C]	150
Operating environment	Chemical industry
Outer PM type	NdFeB
Inner PM type	SmCo
Pullout torque [Nm]	40.3

Table 1 lists the dimension specifications and operating condition to be followed while designing the PMC. Our magnetic coupling is to be installed to drive a chemical pump which is handling an inflammable liquid at a high temperature i.e., 150 °C. The required output torque is 31 Nm at 3450 rpm rated speed. A safety factor of 30 % higher pullout torque than the required output was considered to accommodate the effects of fluid dynamics, after which the target pullout torque was 40.3 Nm at elevated temperature.

The inner and outer diameters of the PMC were fixed due to assembly constraints. Secondary follower part of the PMC is expected to be operating at higher temperature compared to primary driver part, as the former will be more in contact with the liquid at high temperature. Therefore, SmCo magnets were utilized for the follower part of the PMC because they are less affected by the increase in the temperature. NdFeB magnets were utilized for the primary driver as the temperature was expected to be lower on the outer side of PMC; also, NdFeB PMs are cheaper compared to SmCo.

3. 2D and 3D Finite Element Analysis

Generally, 2D FEA is utilized to analyze the performance of radial PMC. 2D FEA simulation time is much lower than 3D FEA; however, it does not consider the end leakage flux of PMC. End leakage flux effect becomes larger when the stack length is shorter as compared to the diameter of the PMC. Furthermore, 2D geometry does not consider the unconventional structures; therefore, the

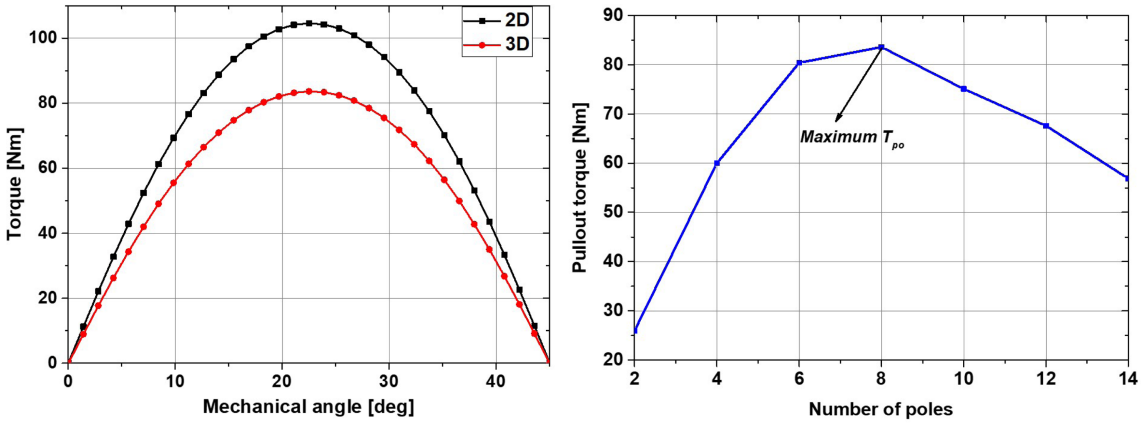

Fig. 2. (Color online) (a) 2D vs 3D FEA (b) No. of poles vs pullout torque.

output cannot be fully reliable. Fig. 2(a) compares the pullout torque of a PMC considering the given dimension constraints and a stack length of 50 mm. The comparison shows that the 2D FEA pullout torque is about 105 Nm compared to 82 Nm when the same model is simulated with 3D FEA. The end effect due to leakage flux becomes more prominent as the ratio of stack length to diameter decreases, therefore 3D FEA was opted for the further analysis.

Generally, PMC pullout torque capability varies as the number of poles are changed. This change is due to the change in dimension and air gap length of the PMC. Therefore, with the given dimension constraints and air gap, an analysis was performed to find the number of poles at which PMC generated maximum torque. Fig. 2(b) shows the comparison of pullout torque with different pole numbers. It is observed that as the number of poles are increased, pullout torque capability of the PMC initially increased and then started reducing; producing maximum pullout torque at number of poles equal to 8.

4. Optimal Design Process

An optimal design process was followed as outlined in Fig. 3 to reduce the PM utilization to fulfill the pullout torque requirement. Firstly, the objective function and the design variables were selected. Then, the Latin Hypercube Sampling (LHS) method was used to design the experiments. After that, the Kriging method was used to approximate the objective function and genetic algorithm (GA) was utilized to find optimal values for the design variables. Finally, transient 3D FEA was carried out to

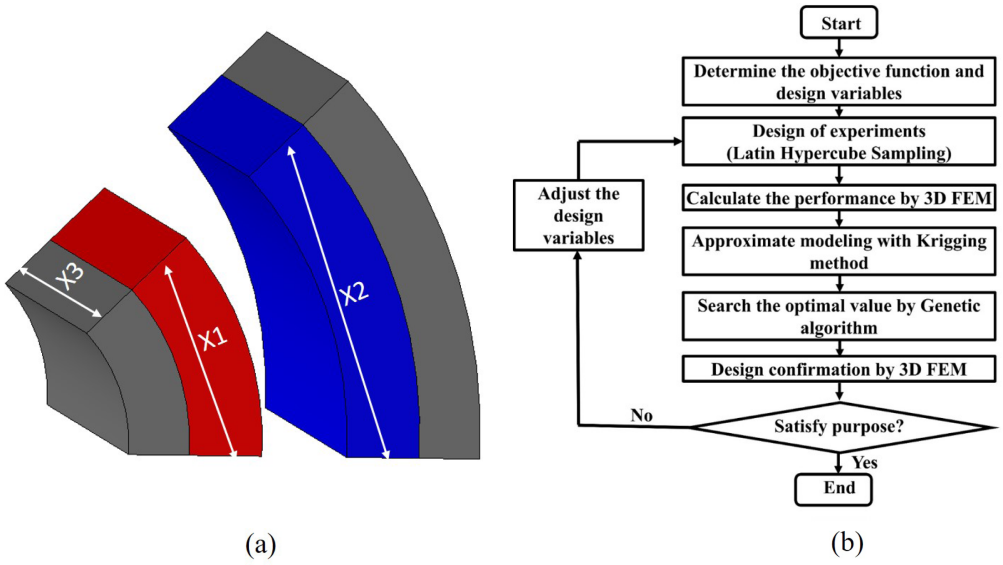

Fig. 3. (Color online) (a) Design variables (b) Optimization process flowchart.

Table 2. Design variables and optimal values.

Item	Variable range	Optimal value
X1 ratio	0.4-0.9	0.752
X2 ratio	0.4-0.9	0.4
X3 [mm]	35-50	49
Max. pullout torque [Nm]	~48	47.8
PM volume [cm^3]	-	260
T/PM volume [cm^3]	-	0.186

verify the output results. Inner and outer diameter of the coupling was fixed due to the space constraints, and the remaining structure was optimized. The design variables are shown in Fig. 3(a), and their range are listed in Table 2.

Inner and outer diameters are fixed and the other variables were optimized to maximize the pullout torque while keeping a minimum of PM volume. Table 2 shows the design variable ranges and values obtained by optimal design process. The ratio, X1 and X2, are the ratio of the PM span to the PM pitch. This value of the ratio will be maximum when PM span is equal to the PM pitch. However, the reduction of these ratios initially does not affect the torque much and therefore, can be optimized to reduce the PM volume for the required torque; which will reduce the overall material [4]. X3 represents the stack length and describes the range and optimal value. Maximum pullout torque was selected to be about 48 Nm, expecting the 7 Nm torque reduction unconventional assembly features.

Figure 4(a) shows the model which is analyzed for the optimal design process. Due to variation in leakage flux as the stack length and PM span changed; a simpler model (Fig. 4(a)) without unconventional assembly parts was optimized and the effect of leakage flux due to assembly geometry was approximated separately. Fig. 4(b) shows the final model with considering unconventional assembly features; iron overhang in stack length direction and between the PMs. As the air gap value is much higher in this PMC, therefore these assembly overhangs cause leakage flux and reduce the torque capability of the coupling.

Figure 5(a) shows the leakage flux due to the PM side and inner assembly iron overhang in the secondary follower of PMC, and Fig. 5(b) shows the same phenomenon in

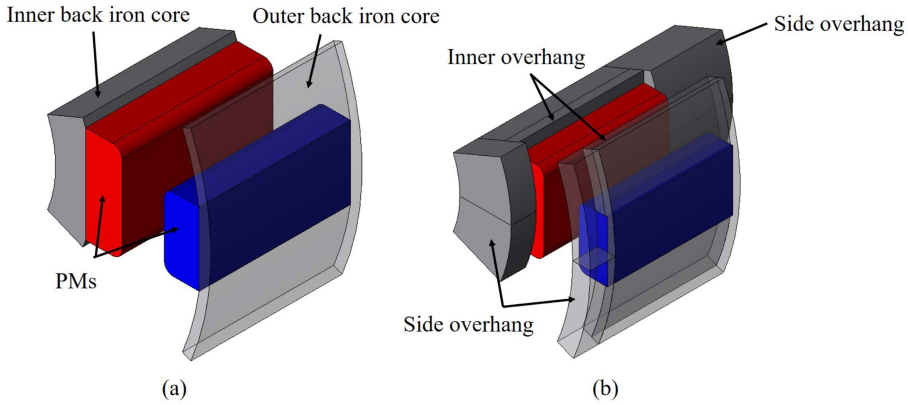

Fig. 4. (Color online) Optimized model (a) Without assembly overhang (b) with assembly overhang.

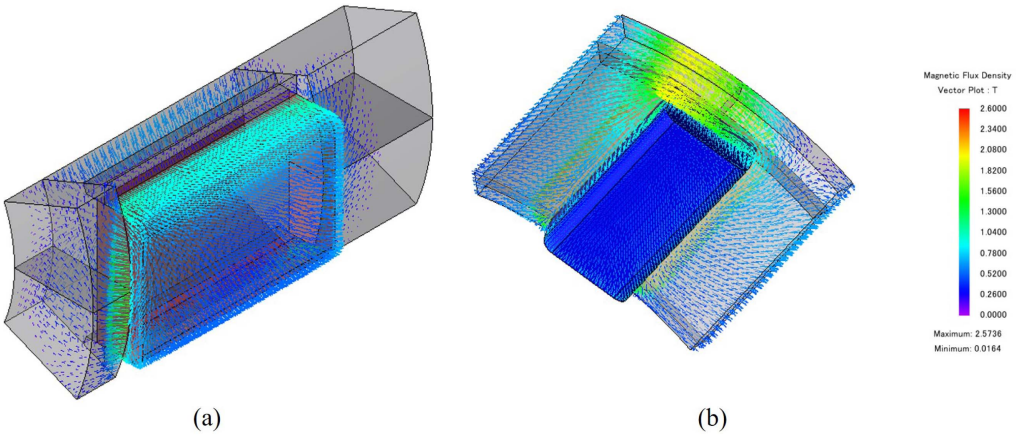

Fig. 5. (Color online) Leakage flux due to assembly geometry (a) Inner part of PMC (b) Outer part of PMC.

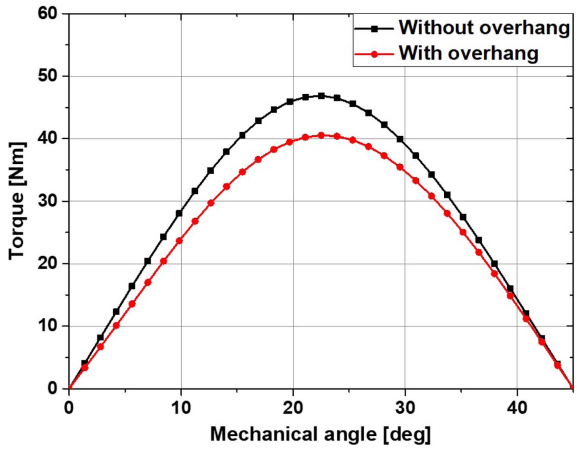

Fig. 6. (Color online) Assembly overhang effect on the pullout torque.

the primary driver. It is observed that many flux vector lines are not crossing the air gap and will cause a reduction in pullout torque. Fig. 6(a) compares that the simpler optimal model without overhang and with overhang due to assembly unconventional structure. A 3D FEA was performed for both models. Firstly, to verify the optimal design process and secondly, to verify if the final model is producing the required pullout torque.

Almost 48 Nm pullout torque, which is same as the target of the optimal design process, was analyzed in the optimal model. Thus, verifying the design process of the PMC with the given constraints of the inner and outer dimensions. Furthermore, when the final model with all the assembly structure was analyzed, it showed a reduction of almost 7.5 Nm of torque, and the final output torque was 40.5 Nm, which is the similar to the required 30 % higher pullout torque i.e. 40.3 Nm. Therefore, it showed that the optimal design process along with leakage flux consideration due to unconventional structure achieved the objective pullout torque.

5. Prototype Manufacture and Testing

To verify the analysis, a prototype was manufactured. Fig. 7 shows various parts of the PMC without the PMs. Fig. 7(a) shows the iron core of the primary mover of the PMC.

It shows the inner assembly and the slots where PMs were inserted. Fig. 7(b) shows the iron core of the secondary follower of the PMC. It also shows the slots for the PM. Fig. 7(c) shows the PMC prototype. The secondary follower has a shaft attached to it while the primary mover is kept fixed during experiment. To analyze the static performance of the PMC, the driving motor rotated the inner secondary follower slowly and the static output

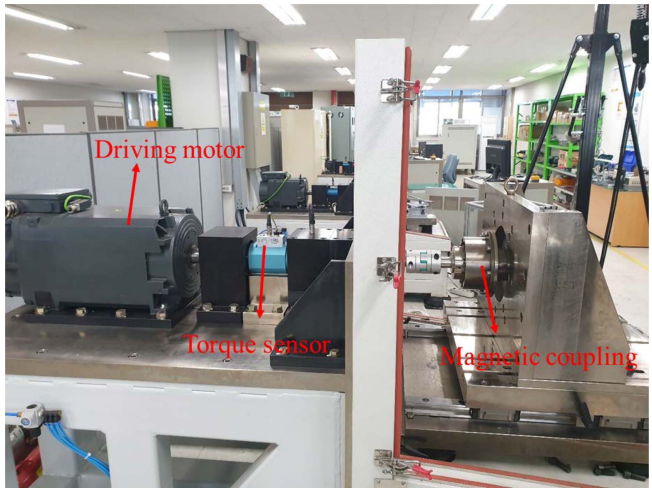

Fig. 8. (Color online) Experimental setup for PMC prototype testing.

(a) (b) (c)

Fig. 7. (Color online) Prototype manufacturing (a) PMC primary mover iron core (b) PMC secondary (c) Prototype PMC.

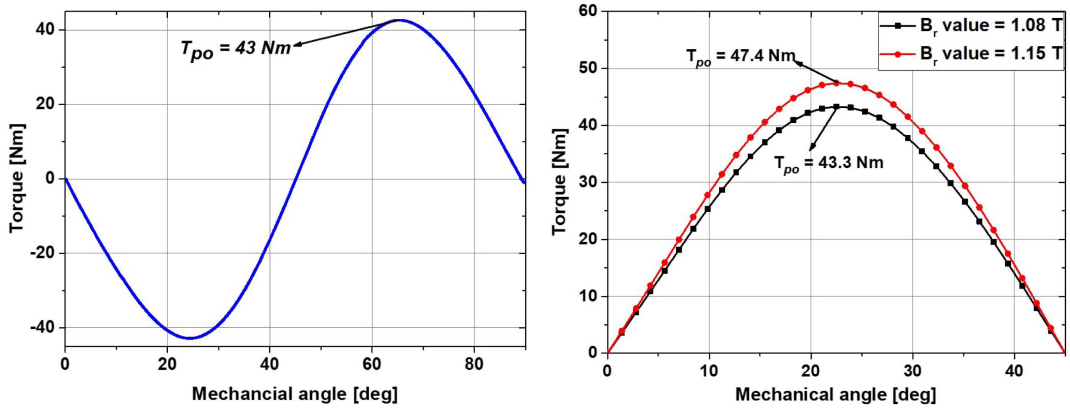

Fig. 9. (Color online) Pullout torque at room temperature (a) Experimental (b) PM B_r value effect on the pullout torque.

torque performance was analyzed with a torque sensor.

Figure 8(a) shows the testing setup for the PMC prototype. It shows that the driving motor is attached to the inner secondary follower while the primary mover is fixed in a jig. We rotated the secondary follower slowly and analyzed the static torque output at room temperature, i.e. 20 ºC. Fig. 9(a) shows the experimental output of the PMC. It shows 43 Nm pullout torque at room temperature, which is 4.4 Nm lower than the simulated value of 47.4Nm at room temperature (Fig. 9(b)). Therefore, we analyzed the B_r value of the permanent magnets that that were in manufacturing. We used YGX-30L SmCo PMs, whose typical Br value is 1.15T, but a minimum Br value could be as low as 1.08 T. We used the typical Br value of SmCo; however, the B_r value of the PMs that were used for manufacturing was 1.08 T. We performed 3D FEA with the corrected Br value and it shows the similar value as the experimental analysis i.e. 43.3 Nm.

Due to the reduced B_r value of the PMs provided by the supplier, there was about 4 Nm reduction in pullout torque. However, after B_r correction, the analyzed pullout torque was verified by the experimental results as shown in Fig. 9.

6. Conclusion

In this paper, a PMC was designed with inner and outer dimension constraints, to be installed in a chemical pump. A 3D finite element analysis was used to optimize the PM volume and maximize pullout torque. Genetic algorithm combined with Latin Hypercube Sampling method was used for the optimization. Then, the optimization results were verified by 3D FEA. Finally, a PMC prototype was built and tested in the laboratory to verify the analysis. A reduction in the Br value of the purchased PMs reduced the static pullout torque ability of the PMC. After correcting the B_r value in the FEA, analysis results verified the experimental results.

Acknowledgments

This work was supported by the Korea Institute of Energy Technology Evaluation and Planning (KETEP) and the Ministry of Trade, Industry & Energy (MOTIE) of the Republic of Korea (No. 20172010106090).

References

[1] W. Wu, H. C. Lovatt, and J. B. Dunlop, IEEE Trans. Magn. **33**, 5 (1997).
[2] R. Hornreich and S. Shtrikman, IEEE Trans. Magn. **14**, 5 (1978).
[3] K. J. Overshott, IEEE Trans. Magn. **25**, 5 (1989).
[4] R. Ravaud, V. Lemarquand, and G. Lemarquand, IEEE Trans. Magn. **46**, 11 (2010).
[5] R. Wang, E. P. Furlani, and Z. J. Cendes, IEEE Trans. Magn. **30**, 4 (1994).
[6] H. J. Shin, IEEE Trans. Magn. **49**, 7 (2013).
[7] S. Högberg, B. B. Jensen, and F. B. Bendixen, IEEE Trans. Magn. **49**, 12 (2013).
[8] R. Ravaud, IEEE Trans. Magn. **45**, 4 (2009).
[9] P. Elies and G. Lemarquand, IEEE Trans. Magn. **34**, 4 (1998).
[10] P. Elies and G. Lemarquand. IEEE Trans. Magn. **35**, 4 (1999).
[11] W. Y. Lin, IEEE Trans. Magn. **44**, 12 (2008).